Analysis of Global Ionospheric Response to Solar Flares Based on Total Electron Content and Very Low Frequency Signals

JIANDI FENG[1,2], BAOMIN HAN[1], FENG GAO[1], TING ZHANG[1], AND ZHENZHEN ZHAO[1]

[1]School of Civil and Architectural Engineering, Shandong University of Technology, Zibo 255000, China
[2]State Key Laboratory of Space Weather, Chinese Academy of Sciences, Beijing 100190, China

Corresponding author: Zhenzhen Zhao (zzzhao@whu.edu.cn)

ABSTRACT The response of the global ionosphere to solar flares is an important topic in the field of space weather. The global ionospheric response to solar flares is comprehensively analyzed from the perspectives of total electron content (TEC) and very low frequency (VLF) signals by using solar flare data on the eruption days of X-class flares from 2006 to 2019, including flare level, flare duration, geographical location, and local time. In addition, the relationship between X-ray flux and VLF phase variation is studied through correlation analysis. The concepts of disturbance intensity (DI) and disturbance angle are defined, and a DI evaluation model is established to help detect the difference in sensitivity to solar flares between TEC and VLF signals. Results show the following. (1) The higher the flare level and the longer the duration, the greater the disturbance to the ionosphere. Simultaneously, a phenomenon exists in which the disturbance caused by low-level and long-lasting flares is greater than that caused by high-level flares. (2) VLF phase variation and flare level exhibit a good correlation, and they are also closely related to geographical location and local time. The disturbance degree of a station facing the sun is more evident than that of a station facing away from the sun. The TEC disturbance of stations in the morning (local time) is more obvious than that in the afternoon, and disturbance increases along the direction of Earth's rotation. (3) When DI is at the same level, the lowest flare level that causes TEC response is higher than the lowest flare level that causes VLF signal response. The disturbance angle of TEC is unevenly distributed within the interval [0°, 90°], and that of VLF signals is more than 85°. The sensitivity of VLF signals to flare response is considerably higher than that of TEC, and the difference between the two even stride across DI level.

INDEX TERMS Disturbance intensity, ionosphere, solar flare, total electron content, very low frequency signals.

I. INTRODUCTION

A solar flare (also known as a chromospheric burst) is a type of high-energy radiation burst phenomenon that is frequently emitted by the sun; it is considered one of the most important types of space weather [1], [2]. In accordance with the magnitude of the peak X-ray flux observed by the Geostationary Operational Environmental Satellite, solar flares can be divided into five levels, and the order of energy is A, B, C, M, and X. The eruption of solar flares will release a large number of high-energy charged particles that are transported to the

Earth through the solar wind. Such eruption is accompanied by an X-ray explosion, which will damage satellites and spacecraft and injure astronauts. In addition, the explosion will seriously affect the quality of radio communication, causing interruptions for several hours and leading to the navigation signal attenuation problem [3]. The ionosphere, which has an altitude of 60–1000 km, is the area where X-rays must pass before reaching the Earth. To determine the disturbance law of the ionosphere during solar flare periods and reduce the damages of solar flares to human life and Earth's environment, research on the response characteristics of the ionosphere to solar flares has always been one of the popular topics among astronomers.

The associate editor coordinating the review of this manuscript and approving it for publication was Prakasam Periasamy.

Ionospheric response to solar flares is mostly attributed to the enhancement of X-ray and extreme ultraviolet (EUV) during solar flares [4]. Enhanced X-ray and EUV during chromospheric bursts can lead to a sudden increase in ionospheric electron density and total electron content (TEC) [5]. In recent decades, related scholars in the field of geophysics have conducted considerable research on the response characteristics of the ionosphere to solar flares. For example, Parmar *et al.* [6] studied the interference mechanism of the C-class flare on July 22, 2016 and the M-class flare on July 23, 2016 in the Indian Regional Navigation Satellite System (IRNSS) signals on the basis of the observed ionospheric TEC data to address the problem of ionospheric ionization enhancement during solar flares interfering with IRNSS navigation signals. Zhang *et al.* [7] investigated the influence factors of solar flare radiation on the response of ionospheric TEC and determined the influence of flare radiation on ionospheric TEC by grouping the X-ray peaks of flares. They found that TEC enhancement is related to the longitude of flares. That is, the larger the longitude, the smaller the TEC enhancement. Moreover, they determined that flare position is an important factor that affects the TEC response intensity of the ionosphere during solar flares. On the basis of the geographical location of an observation station at the time of a flare, Mao *et al.* [8] further examined the response of the equator in the Western Pacific region and the ionosphere in a low-latitude region to the X1.2 solar flare on May 15, 2013. They found that TEC exhibits a significant enhancement and a considerable response only within the vicinity of the geomagnetic equator, proving that the location of a flare exerts an important effect on the response intensity of ionospheric TEC. In addition, the magnitude of a flare is an important factor that affects TEC response during a flare. In ionospheric TEC and its time rate of change curve, information regarding small flares will be completely submerged in background noise and the occurrence of flares cannot be displayed and distinguished. For high-level solar flares similar to the X level, the response of TEC to the flares will be clear and evident [9]. Apparently, the disturbance of TEC can reflect the response of the ionosphere to solar flares to a certain extent.

However, tools for detecting ionospheric response to solar flares are not limited to TEC. Solar flares will also cause a significant increase in daytime ionospheric plasma density and then affect the very low frequency (VLF) signals propagating in the Earth–ionosphere waveguide (EIWG) [10]. EIWG refers to the propagation of VLF signals in a waveguide bounded by the Earth and the low ionosphere [11]. The VLF phase is stable under undisturbed solar conditions, but the variation in electron density and the height distribution in the low ionosphere will lead to the disturbance of the VLF signal propagation mode [12]. The primary reason for the increase in electron density in the ionospheric D-layer during solar flares is the sudden increase in the amount of X-rays [13], [14]. Multiple X-rays emission can increase the electron density of the ionosphere D-layer by 1-2 orders of magnitude, changing

the conductivity at the edge of the upper waveguide along the VLF signal trajectory, and consequently, all the propagation parameters [15]. In addition, VLF signals are highly sensitive to X-ray from solar flares and a close relationship exists between them. X-rays also cause many phase anomalies in VLF signals. For example, the phenomenon of sudden phase anomaly (SPA) in the VLF phase causes abnormal changes; that is, when electron density in the D-layer increases sharply, the equivalent ionospheric reflection height decreases and the VLF signal propagation phase suddenly moves towards the advance phase; this phenomenon is called SPA [16]. The intensity of SPA and X-ray flux exhibit a good correlation.

A large number of studies have shown that a measurement method based on VLF amplitude or phase can be used to detect strong solar flares from the ground, describe their impact near the Earth, and indirectly analyze the properties of solar flares [17]. Ionospheric response to solar flares based on VLF radio signals has also achieved numerous breakthrough results [18]–[20]. For example, George *et al.* [21] studied the long or short wave X-ray flux level by using the VLF phase and amplitude of the NPM Station. They found that the mean squared error of using VLF amplitude to determine long or short waves X-ray flux level is 4–10 times higher than that of using VLF phase. In addition, the sensitivity of VLF signals to solar flares is also reflected in the change in effective reflection height when electron density in the D-layer increases. Vogrinčič *et al.* [22] used the Latin American VLF network receiver station in Mexico City and determined that the phase and amplitude of observed VLF signals decreased significantly when the effective reflection height of the ionosphere's D-layer increased. Palit *et al.* [23] used the amplitude and phase data of VLF signals from the NWC Station. On the basis of their previous model of VLF signal amplitude disturbed by X-class and M-class solar flares, they studied the peak delay of electron density at different altitudes and compared it with the corresponding amplitude delay of VLF signals, obtaining the effective reflection height of VLF signals. Simultaneously, the VLF method is recognized as the only technique for regularly estimating ionospheric D-layer electron density [24].

From the preceding review, TEC data and the VLF method can reflect ionospheric response to solar flares to a certain extent. However, existing research on global ionospheric response to solar flares exhibits the following limitations. (1) Most studies are limited to a single station or a few VLF stations. TEC and VLF data obtained from different geographical locations are considerably different due to the varying characteristics of such locations. The TEC or VLF data of a single station can only reflect local, but not global, ionospheric response to solar flares. (2) Research is only conducted from the perspective of single TEC or VLF data, and thus, lacks the comprehensive response characteristic analysis of both. Single data cannot represent the overall response of the ionosphere to solar flares. Moreover, the sensitivity of the two types of data to X-ray radiation from solar flares considerably differs. A huge difference exists in the

disturbance of TEC and VLF signals caused by flares of the same level. Simultaneously, relevant research on detecting the sensitivity difference between TEC and VLF signals remains lacking. In consideration of the aforementioned limitations, ionospheric TEC data and VLF data provided by the Stanford database are comprehensively used in the current work. Abnormal disturbances of TEC and VLF signals caused by solar flare eruptions under different factors are studied from a global perspective on the basis of the C- to X-class flare data among all the X-class flares from 2006 to 2019. The correlation between X-ray flux and VLF phase variation is also analyzed. In addition, the concepts of disturbance intensity (DI) and disturbance angle are introduced, and a DI evaluation model is established. The sensitivity difference of ionospheric TEC and VLF signals to solar flares is detected, and the response characteristics of the ionosphere to solar flares are identified.

II. DATA AND METHODS
A. IONOSPHERIC TEC DATA
The Global Positioning System (GPS)-TEC algorithm used in this study was proposed by Arikan *et al.* [25] and is called the Reg-Est method. TEC can be calculated for 24 h without interruption by using all the GPS satellite data observed at a station. The time resolution is 30 s. The Reg-Est method is suitable for every station in the middle-, high-, and low-latitude regions of the world, and reliable results can be obtained even when the ionosphere is disturbed. Through relevant tests [26], the Reg-Est method is determined to exhibit good agreement with the code of the International GNSS Service and the calculation results of the Jet Propulsion Laboratory analysis center. After Reg-Est was proposed, relevant scholars [27]–[29] improved this method to make it a more reliable and near to real-time GPS-TEC algorithm [30].

IONOLAB-TEC values are estimated from preprocessed RINEX files [31], [32] using the satellite and receiver bias values, and receiver and satellite locations as follows:

1. Using the inter-frequency satellite bias, IONOLAB-BIAS inter-frequency receiver bias, and pseudorange-leveled baseline phase delay values in the model provided in Nayir *et al.* [28], STEC for every satellite is computed with 30 s time resolution (IONOLAB-STEC).

2. VTEC can be obtained from STEC by the use of a "mapping function" [25], [31], [32]. IONOLAB-STEC is converted into IONOLAB-VTEC by the application of the mapping function provided in Arikan *et al.* [25] for every position of the satellite with a 30 s time resolution.

3. By combining the VTEC for each satellite in the least square sense by employing a weighting function to reduce the multipath effects with an elevation mask of 30°, Reg-Est algorithm is applied to obtain TEC estimates in the form of IONOLAB-TEC with 30 s time resolution as discussed in Arikan *et al.* [27], [28].

At present, the Ionospheric Research Laboratory of the Department of Electrical and Electronics Engineering of Hacettepe University in Turkey provides the application IONOLAB-TEC, which is based on the Reg-Est method and online computing services.

B. VLF PHASE DATA
The Stanford Department of Electrical Engineering developed a space weather detector that can detect changes in Earth's ionosphere caused by solar flares or other disturbances and measure the impact of solar activities (including solar flares) on Earth's atmosphere by observing changes in VLF signals when Earth's ionosphere rebounds. The VLF signal phase data used in the current study are all from the Stanford database (http://sid.stanford.edu/database-browser/). The website provides the location distribution of all monitors in the world, and charts based on the data captured by the monitors, and the time of sunrise and sunset every day with a time resolution of 5 s. The influence of solar flares on the ionosphere is analyzed indirectly by studying the SPA phenomenon of VLF signals.

VLF data acquisition from the Stanford database depends on monitoring stations distributed all over the world. This study selects monitoring stations from different locations worldwide for analysis, including NAA, NML, NLK, NPM, and other stations. Although the working time and data volume of each station in the database differ from one another, VLF phase data from 2006–2019 can be obtained relatively complete from global monitoring stations. In VLF data processing, the superposition effect of successive solar flares on VLF signal phase data should be considered, this study further selects VLF data in which the time interval between two flares is greater than 0.5 h when detecting sensitivity difference to solar flare between TEC and VLF signals.

C. X-CLASS SOLAR FLARES DATA
The detailed information of C-class to X-class solar flares in the last 20 years has been recorded in the solar activity prediction center platform of the National Astronomical Observatories of the Chinese Academy of Sciences (https://tesis.lebedev.ru/en/sun_flares.html?m=9&d=10&y=2017). In this study, solar activity data from 2006 to 2019 are classified and processed using the platform. This paper only shows the data of X-class flares from 2006 to 2019 (Table 1) due to page limitation. In the table, "omitted" indicates missing data.

III. RESPONSE ANALYSIS OF TEC AND VLF SIGNALS TO SOLAR FLARES
A. RESPONSE ANALYSIS OF IONOSPHERIC TEC TO SOLAR FLARES
Solar flares that generate a strong response in ionospheric TEC are mostly X-class flares. For example, the NKLG Station observed two X-class flares on September 6, 2017, namely, the X2.2 flare at 08:57–09:17 UT and the X9.3 flare at 11:53–12:10 UT. In addition, several M-class flares broke out in the morning of October 28, 2013 (local time) at the

TABLE 1. X-class solar flares in 2006–2019.

Release time	Time	Flare level	Release time	Time	Flare level
December 5, 2006	10:18 UT	X9.0	November 5, 2013	22:07 UT	X3.3
December 6, 2006	18:29 UT	X6.5	November 8, 2013	04:20 UT	X1.1
December 13, 2006	02:14 UT	X3.4	November 10, 2013	05:08 UT	X1.1
December 14, 2006	21:07 UT	X1.5	November 19, 2013	10:14 UT	X1.0
February 15, 2011	01:44 UT	X2.2	January 7, 2014	18:04 UT	X1.2
March 9, 2011	23:13 UT	X1.5	February 25, 2014	00:39 UT	X4.9
August 9, 2011	07:48 UT	X6.9	March 29, 2014	17:35 UT	X1.0
September 6, 2011	22:12 UT	X2.1	April 25, 2014	00:17 UT	X1.3
September 7, 2011	22:32 UT	X1.8	June 10, 2014	11:36 UT	X2.2
September 22, 2011	10:29 UT	X1.4	June 10, 2014	12:36 UT	X1.5
September 24, 2011	09:21 UT	X1.9	June 11, 2014	08:59 UT	X1.0
November 3, 2011	20:16 UT	X1.9	September 10, 2014	17:21 UT	X1.6
January 27, 2012	17:37 UT	X1.7	October 19, 2014	04:17 UT	X1.1
March 5, 2012	02:30 UT	X1.1	October 22, 2014	14:02 UT	X1.6
March 7, 2012	00:02 UT	X5.4	October 24, 2014	21:07 UT	X3.1
July 6, 2012	23:01 UT	X1.1	October 25, 2014	16:55 UT	X1.0
July 12, 2012	15:37 UT	X1.4	October 26, 2014	10:04 UT	X2.0
October 23, 2012	03:13 UT	X1.8	October 27, 2014	14:12 UT	X2.0
May 13, 2013	01:53 UT	X1.7	November 7, 2014	16:53 UT	X1.6
May 13, 2013	15:48 UT	X2.8	December 20, 2014	00:11 UT	X1.8
May 14, 2013	omitted	X3.2	March 11, 2015	16:11 UT	X2.1
May 15, 2013	01:25 UT	X1.2	May 5, 2015	22:05 UT	X2.7
October 25, 2013	07:53 UT	X1.7	September 6, 2017	08:57 UT	X2.2
October 25, 2013	14:51 UT	X2.1	September 6, 2017	11:53 UT	X9.3
October 28, 2013	01:41 UT	X1.0	September 7, 2017	14:20 UT	X1.3
October 29, 2013	21:42 UT	X2.3	September 10, 2017	15:35 UT	X8.2

ISPA Station. These flares caused considerable disturbance to ionospheric TEC. Figure 1 shows the disturbance of TEC at the NKLG and ISPA Stations in the two aforementioned days.

As shown in Figure 1(a), the TEC of the ionosphere exhibits different degrees of enhanced response during the outbreak time of the X-class flares with levels X2.2 and X9.3. Given the size of the X-ray flux, the TEC disturbance rate of the former is evidently smaller than that of the latter. On the basis of the difference between the TEC data at the moment of flare eruption and the data when TEC reaches maximum disturbance after the flare ends, a conclusion can be drawn that the enhanced response of TEC to the X2.2 and X9.3 flares in Figure 1(a) is approximately 2.37 TEC unit (TECU) and 3.10 TECU, respectively. The higher the flare level, the greater the effective X-ray flux, and the greater the disturbance to TEC. The NKLG Station (0.4°N, 9.7°E) is located in East Area 1. After converting to local time and

combined with Figure 1(a), the observation station was facing the sun from 06:00 to 18:30 local time, and the TEC value exhibited evident and frequent disturbances. During the period of 06:00–14:00 local time, the station gradually began to face the sun from the back, and TEC exhibited a continuous increase. During the period of 14:00–18:30 local time, the station gradually turned away from the sun, and TEC demonstrated a continuous decline. During the flare, X-rays caused significant ionization enhancement in the ionosphere on the sunward side, but only slight ionization enhancement on the backside. This result is consistent with the explanation provided by Bahari *et al.* [33] for TEC decline during a flare period. That is, the local time of a station is closely related to TEC disturbance during a solar flare.

The ISPA Station (27°S, 109°W) in Figure 1(b) is located in West Area 7. At approximately 12:30 UT, the ISPA Station began to change its position from the backside to the sunward side. Several M-class flares broke out at
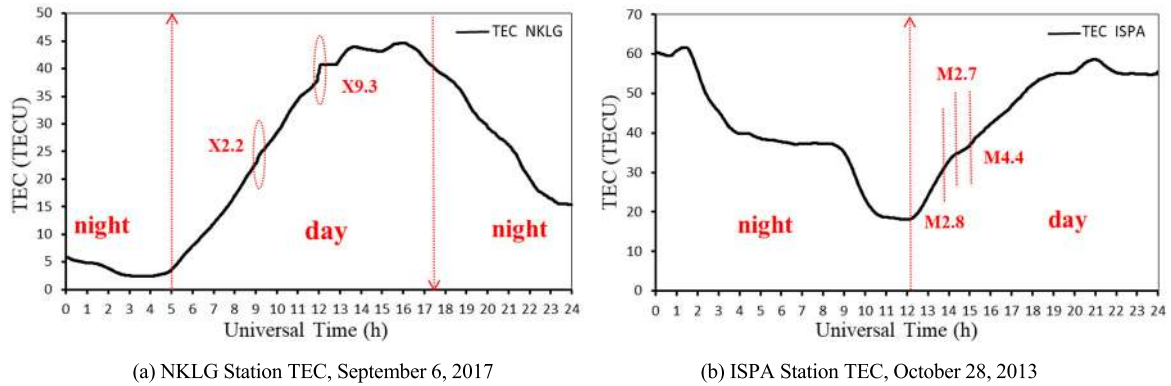
(a) NKLG Station TEC, September 6, 2017   (b) ISPA Station TEC, October 28, 2013

FIGURE 1. TEC images of the NKLG and ISPA Stations during the flare.

14:00–16:00 UT, causing continuous and enhanced disturbance of TEC. Among these flares, the duration of the M2.8 flare at 14:00–14:12 UT was 12 min, and the disturbance of TEC (DTEC) was approximately 1.32 TECU. Meanwhile, the duration of the M2.7 flare at 14:46–15:04 UT was 18 min, and DTEC was approximately 1.5 TECU. When the flare level is close to that of the burst time, the duration of the flare will be longer, the temporal change rate and cumulative variation of TEC will be greater, and the response of TEC to the flare will be stronger. This conclusion is consistent with the result of the statistical analysis conducted by Chen *et al.* [34] of TEC's sudden enhancement caused by the 1996–2003 large flare events, reflecting the correctness of Chapman's ionization theory. Simultaneously, the disturbance caused by low-class flares is greater than that caused by short-term high-class flares providing that the duration is long. Smaller flares may also lead to a higher temporal variation rate of TEC. This finding is consistent with the problem and conclusion drawn by Leonovich *et al.* [35] when TEC changed considerably while the flare level was small at the BRUS and BAHR GPS Stations. In addition, the comprehensive analysis of Figure 1 shows that the effect of solar flares on the ionosphere in the aforementioned stations differs due to the influences of longitude, latitude, and local time. The effect of large flares above X-class on ionospheric TEC is evident, but that of M-class and below flares is relatively weak.

The two images in Figure 1 show that the geographical location of an observation station is closely related to the disturbance of ionospheric TEC during flare eruption. To detect the response characteristics of TEC to flares in different geographical locations, this study uses the X1.6 flare that broke out on November 7, 2014 as an example. Considering that the distribution of TEC stations is relatively scattered and a small number of station data loss phenomena occur, we select West Areas 4–6, where TEC stations are more densely distributed, as the study area. We choose 26 stations with relatively complete data in the Northern and Southern Hemispheres to study the disturbance characteristics of ionospheric TEC at different latitudes. The longitude and latitude

data of the TEC stations in each time zone are provided in Table 2.

On November 7, 2014, the eruption time of the X1.6 flare was 16:53–17:34 UT and the duration was 41 min. After converting to the local time of West Area 5, this period was around 12:00, and the sun was shining at approximately 75°W. Setting West Area 5 as the central time zone and combining the cooperative difference method, the TEC perturbations in the latitude and longitude directions of each time zone are obtained by sampling a time zone from the west and the east respectively (Figure 2). Given the limited number of TEC stations, the DTEC level within the range of 77°N–45°S is shown in West Area 5, and only the DTEC level in the Northern Hemisphere is provided in West Areas 4 and 6. The DTEC of the GLPS Station in the Southern Hemisphere is used to supplement the DTEC near the equator of West Area 6.

As shown in Figure 2, when the sun is directly directed at West Area 5, the equatorial and high-latitude regions in this area exhibit an abnormal TEC enhancement. DTEC decreases gradually from the equator to the mid-latitude, and this phenomenon may be related to a change in the solar zenith angle. The enhancement amplitude of TEC will be considerably reduced with an increase in the solar zenith angle [36]. However, the maximum variation range of the solar zenith angle is approximately 47°, and thus, DTEC exhibits a continuous increasing trend from mid-latitude to high latitude. Meanwhile, the Southern Hemisphere presents a decreasing trend from the equator to Antarctica. When the solar flare erupted, the local time of West Area 4 was in the afternoon and that of West Area 6 was in the morning. The DTEC levels of the two time zones exhibit an opposite trend from the equator to the high-latitude region. The ionospheric TEC of West Area 4 presents an overall increase from the equator to the polar region, whereas that of West Area 6 shows an overall decrease. When the solar flare broke out, the local time of West Area 5 was at noon. By comparing the DTEC levels of West Areas 4 and 6, we find that the response of TEC to the flare burst in the morning of the local time is considerably greater than that in the afternoon of the local

TABLE 2. Longitude and latitude information of selected TEC stations in west areas 4–6.

| Time Zone	TEC Station	Latitude and Longitude	TEC Station	Latitude and Longitude
West Area 4	Alrt	$82°N, 62°W$	Hlfx	$45°N, 63°W$
	Nain	$56°N, 62°W$	Brmu	$32°N, 64°W$
	Sch2	$54°N, 67°W$	Cro1	$17°N, 64°W$
	Escu	$47°N, 64°W$		
West Area 5	Thu3	$77°N, 69°W$	Riop	$2°S, 78°W$
	Baie	$48°N, 68°W$	Areq	$16°S, 71°W$
	Barh	$44°N, 68°W$	Iqqe	$20°S, 70°W$
	Wes2	$42°N, 71°W$	Copo	$27°S, 70°W$
	Bogt	$5°N, 74°W$	Coyq	$45°S, 71°W$
West Area 6	Reso	$75°N, 95°W$	Nlib	$41°N, 92°W$
	Bake	$64°N, 96°W$	Ssia	$18°N, 89°W$
	Chur	$59°N, 94°W$	Mana	$12°N, 86°W$
	Picl	$51°N, 90°W$	Glps	$1°S, 90°W$
	Dubo	$50°N, 96°W$		
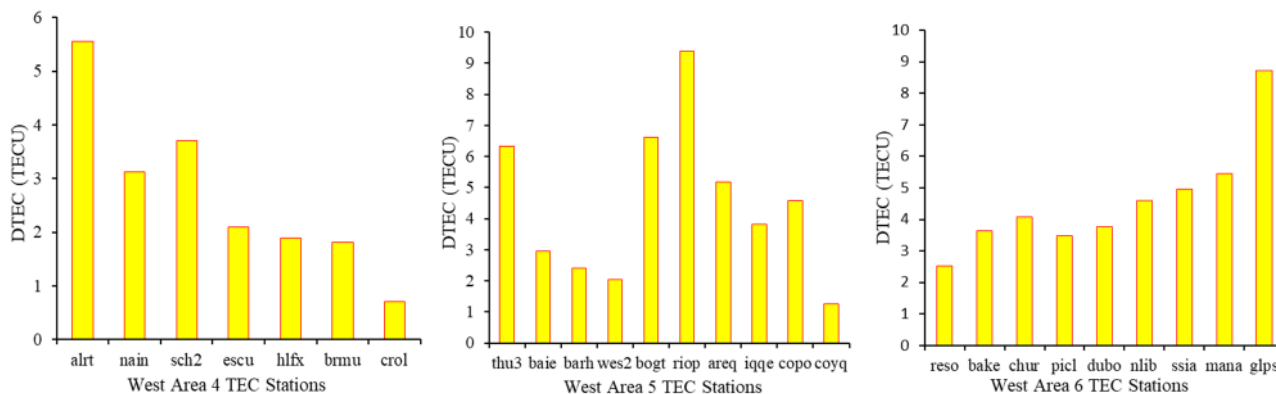
FIGURE 2. TEC disturbance in West Areas 4–6 during the X1.6 flare on November 7, 2014.

time. In addition, from the change trend of DTEC from West Areas 4 to 6, we can infer that DTEC is closely related to the longitude of a station, and TEC increases gradually from West Areas 4 to 6. Zhang et al. [7] selected a study area in the Eastern Hemisphere. Through the grouping analysis of X-ray peak levels, they concluded that the greater the longitude, the smaller the TEC enhancement. In the current work, the study area is set in the Western Hemisphere, and the changes in DTEC level with longitude are investigated. Combined with the conclusion of the Eastern Hemisphere, we determine that the DTEC level is closely related to the longitude of a station, exhibiting an increasing trend in the direction of Earth's rotation.

B. RESPONSE ANALYSIS OF VLF SIGNALS TO SOLAR FLARES

During a solar flare, many factors affect VLF signal strength, such as the duration of the flare and the flare level. Using the

flare that broke out on May 5, 2015 as an example, this study investigates the response of VLF signals to solar flares from the perspectives of flare duration and level. A total of 23 solar flares, including 4 M-class and 1 X-class large-scale flares, broke out on that day. Figure 3 shows the disturbance to the VLF signals caused by the solar flares.

As shown in Figure 3, the phase of VLF signals exhibit different degrees of response to flares above the M level, and the sudden disturbance caused by the X2.7 flare burst at 22:05 UT is the greatest. In addition, the VLF phase is disturbed obviously by the C-class flares which are continuously erupting and lasting for a long time. It can be seen that the duration of the flare is closely related to the abnormal disturbance of the VLF. In Figure 3, the level of the C3.7 flare at 08:20–08:37 UT is lower than that of the M1.9 flare at 09:42–09:47 UT. However, the duration is 3.4 times that of the latter, and the impact on VLF signals is significantly greater than that of the latter. This finding shows again that the
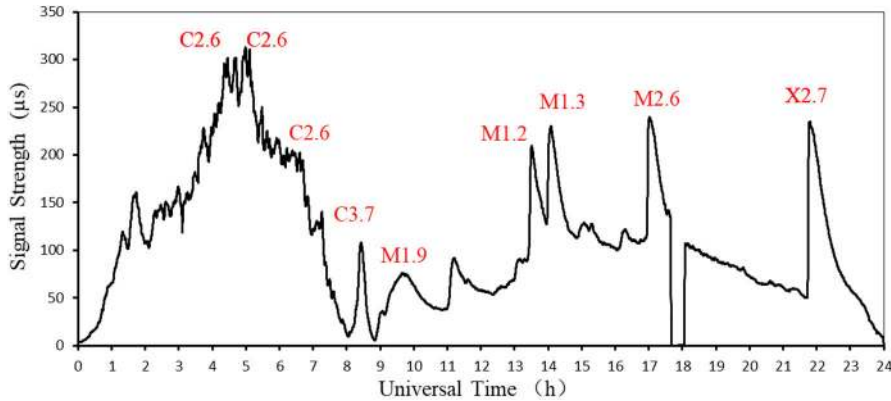
FIGURE 3. VLF phase image of the NAA-N2JUP Station on May 5, 2015.

duration of a flare is an important factor in disturbing the VLF phase. The influence of low-level flares with long duration on VLF is also greater than that of high-level flares. Because the abnormal change of VLF phase is not only related to the duration of the flare, but also to the level of the flare and the geographical location of the observation station in the flare burst period. That is to say, even if the two levels are the same and the flare duration is different, their respective disturbance to VLF phase can not only be attributed to the different duration of the flare, because the location of the station at the flare burst time will also have an important influence on the phase disturbance momentum, it is impossible to separate other factors, and the absolute relationship between the magnitude of abnormal disturbance momentum and the flare duration can be determined. Considering that the duration of a flare mostly affects the total amount of VLF phase anomaly, this study defines the total disturbance F of VLF phase anomaly as the function $\varphi(t)$ of time t, and the simple calculation formula for F is given as follows:

$$F = \int_{begin}^{end} \varphi - \varphi(begin)dt \qquad (1)$$

where *begin* refers to the start time of the flare, *end* refers to the end time of the flare, and $\varphi(begin)$ refers to the normal fluctuation phase of VLF signals during flare eruption. Eq. (1) shows that the longer the flare duration, the larger the total amount of VLF phase abnormal disturbance, and the longer it takes for the phase to return to normal.

Excessive solar X-ray radiation during solar flares increases ionospheric D-layer ionization, affecting the amplitude and phase of VLF signals in the lower ionosphere [37]. In Figure 3, the M1.2 flare at 13:45 UT burst and the M1.3 and M2.6 flares successively caused large disturbances to the VLF phase, and the magnitude of the disturbance presents an upward trend. This result is consistent with the order of flare levels. Initially, the larger the flare level, the greater the disturbance to VLF signals. The flare level is measured in accordance with X-ray flux density. To further explore the relationship between flare level and VLF signal disturbance, the relationship between flare level and VLF phase variation

is obtained using all the available data of X-class flares from 2006 to 2019, combined with a linear regression analysis method. The results are presented in Figure 4.

From left to right and from top to bottom of Figure 4, the stations used are distributed in the low, middle, and middle latitudes of the Northern Hemisphere and high latitudes of the Southern Hemisphere. The X-rays emitted from a solar flare propagate at the speed of light and reach the Earth after 8 min and 18 s. In accordance with the time of X-class flare eruption, the corresponding time of the VLF data obtained from the Stanford database is postponed by 8 min and 18 s. After the maximum value of disturbance is detected, the variation in VLF disturbance is calculated using a difference method. Combined with the correlation analysis, the Pearson correlation coefficients between flare level and VLF disturbance are 0.942, 0.916, 0.924, and 0.952; and the correlation degree is above 0.9. A good correlation exists between flare level and VLF disturbance; that is, the larger the flare level, the greater the disturbance to VLF signals. The result is consistent with the conclusion obtained by Hayes *et al.* [38] on the correlation between differential VLF and flare X-ray flux. However, the assumption that VLF disturbance caused by long-lasting low-level flares is greater than that caused by high-level flares cannot be ruled out. From the perspective of the VLF phase disturbance degree of the four subgraphs in Figure 4, we can infer that the response of VLF signals to solar flares exhibits a gradual increase from low latitudes to middle and high latitudes on a global scale. The disturbance of VLF signals due to flares tends to increase with an increase in latitude.

In this work, while studying the influences of flare duration and X-ray flux of flare radiation on VLF signal disturbance, we also determine the influences of the geographical location and local time of different stations on VLF disturbance during flare occurrence. Using the NAA and NPM Stations of RoswellMeteor on March 11, 2015 as examples, the VLF disturbances of the two stations are described in Figure 5.

As shown in Figure 5, the response of VLF signals in different stations to solar flares exhibits evident differences. The response of the VLF signals (green curve) of the NAA Station of Roswell Meteor to solar flares is significantly greater than
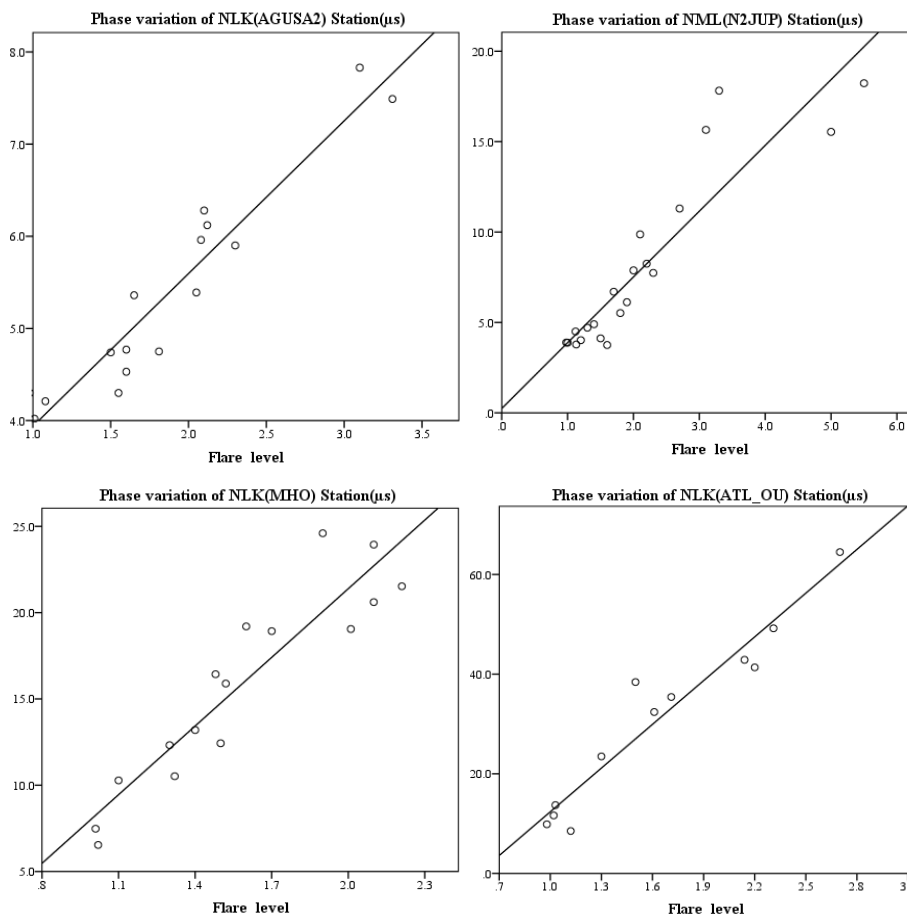
FIGURE 4. Linear regression analyses of flare level and (VLF) phase change.
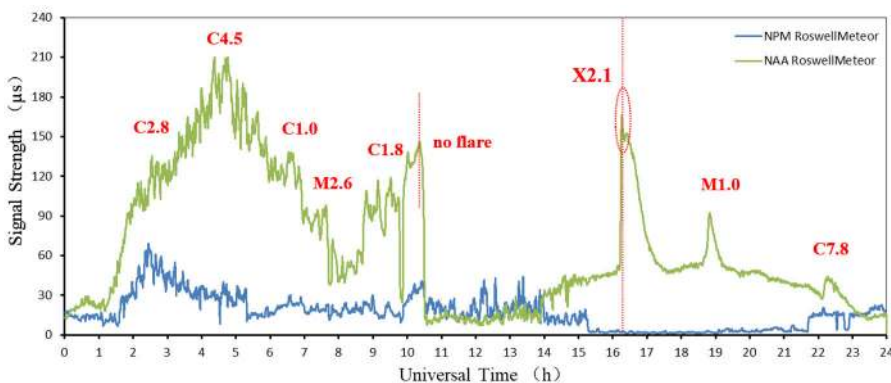

FIGURE 5. VLF images of the NAA and NPM Stations on March 11, 2015.

that of the NPM Station (blue curve). If VLF signals strength changes at daytime, then this phenomenon is called sudden ionospheric disturbance (SID). During SID, the number of ionized particles in the ionosphere will increase or decrease, and thus, VLF radio waves will be more or less reflected [39]. As shown in Figure 5, VLF signals have several sudden disturbances during daytime, e.g., the disturbance caused by

the X2.1 flare at 16:11 UT explosion, but the VLF signals of the NAA and NPM Stations of Roswell Meteor produce completely different responses. The reason for this phenomenon is that Roswell Meteor (33.4°N, 104°W) is located in West Area 7, and the Coordinated Universal Time (UTC) of the NAA Station is not offset. Therefore, 16:11 UT is directly converted into local time, which is 11:13, indicating that the
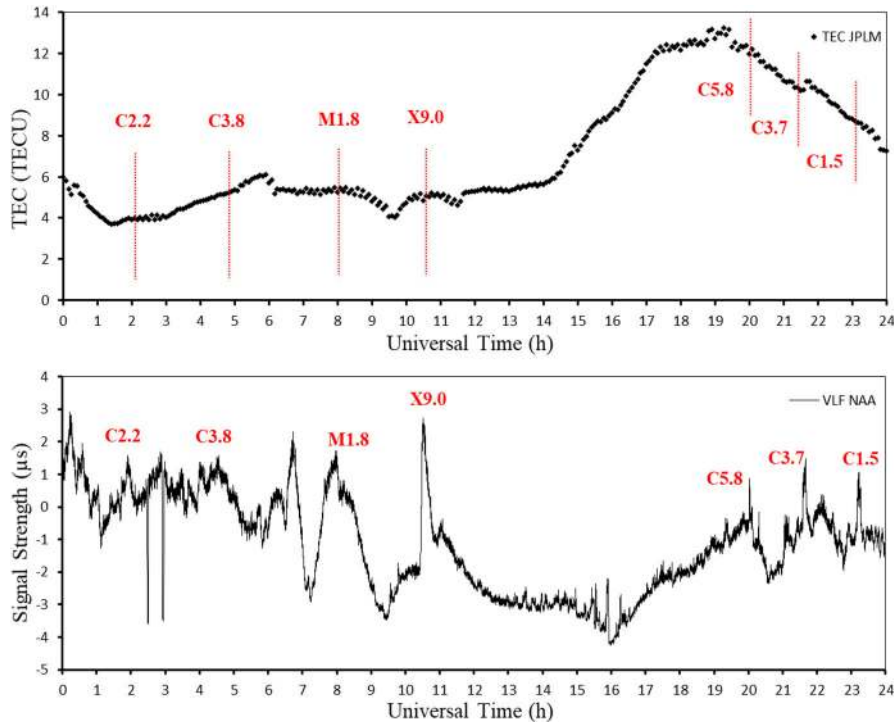
NAA Station is in the solar direction at this time, and the VLF signals exhibit evident phase anomaly. The UTC offset of the NPM Station is 18 time zone. Pushing West Area 7 forward, the 18 time zone is East Area 11, and the local time was 03:13 on March 12, 2015, indicating that the NPM Station was at the back of the sun at this moment, and VLF signals exhibited no phase abnormality. The results show that the disturbance caused by solar flares during daytime is considerably greater than that caused by flares of the same level at night. Geographical location and local time are important factors that affect VLF signal phase. In addition, although no flare occurred at the time marked "no flare" with red line in Figure 5, VLF signals also exhibit certain disturbance. This finding proves that factors that affect signal disturbance are not only solar flares during solar activities, but also other factors, such as lightning and other weather disturbances. By contrast, a large number of flares occasionally occur, but interference to VLF signals is extremely weak probably due to VLF data being located at the backside of the Earth; this phenomenon may also be related to the geomagnetic effect [40].

C. COMPREHENSIVE ANALYSIS OF THE RESPONSE OF TEC AND VLF SIGNALS TO SOLAR FLARES

A certain relationship exists between ionospheric TEC and VLF signals and solar flares. To explore the specific relationship between TEC and VLF signal abnormal disturbance, this study uses the flare that broke out on December 5, 2006 as an example to conduct further longitudinal comparative analysis. A total of 11 flares broke out during that day. Among

which, the X9.0 flare exhibited the greatest impact. TEC and VLF signals exhibited evident changes, as shown in Figure 6.

As shown in Figure 6, although the levels of the C5.8 and C3.7 flares that burst successively at 19:49 UT are relatively low, the duration of the flares is long, and the continuous bursts cause a continuous decrease in and instantaneous enhancement of TEC and VLF signals, respectively. The X9.0 flare is a typical needle-shaped single peak. The disturbance to the VLF signals of the ionosphere is characterized by instantaneous enhancement, short flare duration, insufficient ionization of the low ionosphere, and the end of flare before TEC content changes. This characterization fitly explains that TEC is less sensitive to solar flares than VLF signals. In addition, the analysis of VLF images from the perspective of time effectively verifies the conclusion that the disturbance of VLF signals caused by flares in the morning is frequently greater than that in the afternoon. By comparing the responses of TEC and VLF signals to solar flares in Figure 6, different levels of flares cause varying disturbance changes to VLF signals. The VLF images show that the responses to flares are mostly needlelike single peaks. Meanwhile, the TEC images present gentle slope responses. In Figure 6, when the M1.8 flare at 07:45 UT and the X9.0 flare at 10:18 UT exert extremely weak influences on ionospheric TEC, the VLF phase produces large disturbances, indicating that VLF signals can reflect the response characteristics of the ionosphere more accurately than TEC.

To further explore and analyze the sensitivity difference to solar flares between TEC and VLF signals, this study defines the global disturbance effect on TEC and VLF signals during solar flare eruptions as DI. The angle between the direction

of the line between the initial and maximum values of the disturbance and the X-axis of the coordinate system is defined as the disturbance angle (θ). The magnitude of DI is closely related to disturbance quantity, but the measurement index of DI cannot only depend on the magnitude of disturbance. Therefore, on the basis of the disturbance momentum, this study introduces the influence of the disturbance rate (v) on DI and defines it as a function of flare duration t and disturbance angle θ. The specific gravity of each disturbance angle is obtained by turning the magnitude of each disturbance angle to the vertical angle. The v value is limited within the interval [0, 1], constraining the unidirectional influence of disturbance momentum on DI and reflecting the DI of solar flares on the TEC and VLF signals of the ionosphere. The evaluation model of DI (Eq. (2)) is established on the basis of this idea.

$$
\begin{cases}
DI_V = v(V_{\max} - V_{beg}) \\
DI_T = v(T_{\max} - T_{beg}) \\
v = \theta_{V,T}/90 \\
\theta_V = arctan(V_{\max} - V_{beg})/(t_{\max} - t_{beg}) \\
\theta_T = arctan(T_{\max} - T_{beg})/(t_{\max} - t_{beg})
\end{cases}
\tag{2}
$$

where DI_V is the DI of a flare to TEC (unit: TECU); DI_V is the DI of a flare to VLF signals (unit: μs); V_{beg} and T_{beg} refer to the initial disturbance values of VLF signals and TEC, respectively; $V_{\max}$ and $T_{\max}$ refer to the maximum disturbance values of VLF signals and TEC, respectively; t_{beg} and $t_{\max}$ refer to the starting and peak times of the disturbance, respectively; and θ_V and θ_T refer to the disturbance angle of VLF signals and TEC, respectively.

To obtain the lowest flare level that can produce the response of TEC and VLF signals and then compare the quantitative sensitivity difference between them when the DI of solar flares is equal to one another, this study uses the TEC data of all the X-class flare eruption days and all available VLF data from 2006 to 2019 to detect and analyze the sensitivity difference between TEC and VLF signals. Considering that data will vary considerably due to different geographical locations, the TEC and VLF data used in this study are from the JPLM Station (34°N, 118°W) and the TSOJAI NML Station (34°N, 119°W), with similar geographical coordinates in West Area 8, to reduce the influences of geographical location and local time factors on DI. The time interval of successive flares is short and exerts a superimposed disturbance effect on TEC and VLF signals. Thus, we further select the TEC and VLF data with the time interval of two flares longer than 0.5 h. The average value of multiple disturbance intensities obtained at the same flare level is set as the final value. The obtained TEC and VLF disturbance intensities (DIT and DIV) are presented in Figure 7.

As shown in Figure 7, VLF signals exhibit a strong response to the C-class flare stage, and the disturbance range is C–X. The DI caused by flares to VLF signals increases with an increase in flare level. The minimum value of DIV is 4.51 μs, and the maximum value is 57.55 μs. However,
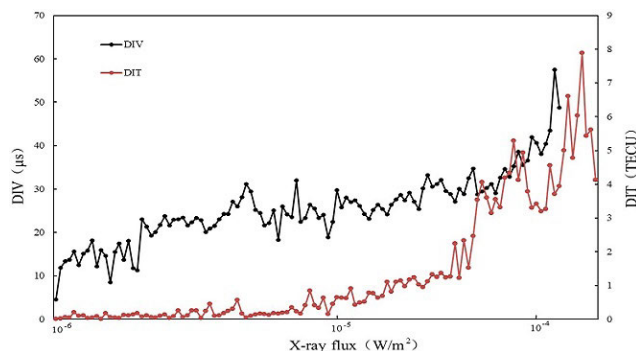

FIGURE 7. Comparison of the DI of solar flares to VLF signals and TEC.

the C-class flare stage of TEC is always in a low state, and the DIT value does not change significantly until the stage between C and M is crossed. The DIT value starts increasing, indicating that TEC gradually generates a strong response to solar flare disturbance, and the disturbance range is from M to X. From the change curve of TEC in Figure 7, TEC also exhibits a certain degree of response to several high-level and long-lasting C-class flares. The minimum value of DIT is 0.006 TECU, and the maximum value is 7.88 TECU. Combined with the DI value variation range of TEC and VLF signals, DI is divided into four intensity levels, namely, W, S, I, and A, in accordance with the following order: weak disturbance, strong disturbance, intense disturbance, and acute disturbance (the units of DIT and DIV are TEC and μs, respectively). After further sorting and classification of DI values, the lowest flare level causing the same DI between TEC and VLF signals is obtained. The results are provided in Table 3.

TABLE 3. Lowest flare level of TEC and VLF signals responding to each DI level.

DIT	DI class	Min flare class	DIV	DI class	Min flare class
0.08<DIT≤ 1.03	W	C1.4	4.51<DIV≤ 14.38	W	C1.0
1.03<DIT≤ 3.31	S	M2.6	14.38<DIV≤ 28.76	S	C1.4
3.31<DIT≤ 5.42	I	M7.0	28.76<DIV≤ 43.16	I	C5.8
DIT>5.42	A	X1.7	DIV>43.16	A	M9.4

From Table 3, the lowest level of solar flares causing S-level disturbance in TEC is M-level flares, and the lowest level of solar flares causing S-level disturbance in VLF signals is C-class flares. When DI level is the same, the lowest level of TEC responding to solar flares is greater than that of VLF signals, and the response of TEC to solar flares exhibits a certain lag. By contrast, VLF signals exhibit strong sensitivity. The response of VLF signals to smaller flares is frequently equivalent to TEC's response to larger flares, and the response gap between VLF signals and TEC even

exceeds the DI level. In Table 3, the DI of the C1.4 flare to TEC reaches W level and that to VLF signals reaches S level. The sensitivity difference between the two to flare response reaches the level of crossing intensity, proving the strong sensitivity of VLF signals to solar flares. The DI detected in this study comprehensively considers disturbance quantity and disturbance rate. Disturbance rate depends on disturbance angle. While studying the influence of disturbance angle on the sensitivity of VLF signals, disturbance angle is found to make a strong contribution to the sensitivity of VLF signals, as shown in Table 4.

TABLE 4. Statistical analysis of the distribution of disturbance angle between TEC and VLF signals.

θ	Quantity (TEC)	Percentage (TEC)	Quantity (VLF signals)	Percentage (VLF signals)
$0° \leqslant \theta \leqslant 15°$	8	6.7%	0	0
$15° < \theta \leqslant 40°$	25	20.8%	0	0
$40° < \theta \leqslant 75°$	54	45%	0	0
$75° < \theta \leqslant 90°$	33	27.5%	112	100%

From Table 4, the disturbance angles of TEC are unevenly distributed within the interval [0°, 90°], The frequency of the disturbance angle within [40°, 75°] is the highest, reaching 45%. Given the strong response of TEC to M-class and X-class flares, the frequency of disturbance angle appearing within the interval [75°, 90°] is relatively high, but the frequency of the disturbance angle less than 75° is as high as 72.5%, restricting the disturbance rate and causing the entire TEC image to present a gentle slope. However, the disturbance angle of VLF signals is mostly distributed within [75°, 90°]. The actual data show that the disturbance angle of VLF signals is above 85°, and the disturbance rate is extremely high. Therefore, the entire image of VLF signals shows an instantaneous enhancement and decline of vertical variation. Meanwhile, the VLF signals' disturbance angle is close to vertical and highly concentrated, which can explain the phenomenon in which most VLF images show a needlelike single peak, reflecting the important contribution of disturbance angle to disturbance rate and DI. The lowest flare level that causes TEC and VLF signals to respond to solar flares under the same DI and the distribution of their disturbance angles show that VLF signals are considerably more sensitive to solar flares than TEC, and the sensitivity difference between the two can even reach the level of equivalent response after crossing the intensity level.

Using the multiple flares that broke out on March 9, 2011 as an example, this study randomly selects the TEC of the ULAB Station and the VLF signals of the NLK Station to verify further the conclusion of difference in sensitivity. The X1.5 flare occurred on that day. The two subgraphs in Figure 8 describe the response of the TEC of the ULAB Station and the VLF signals of the NLK Station to the afore-mentioned solar flare.

From the image of the VLF signals in Figure 8, the C4.7 flare at 02:48–03:26 UT, and the subsequent C6.4, C9.4, M1.7, C5.0, C9.4, and X1.5 flares that successively erupted in the evening exhibited an evident interference on VLF signals. However, only the M1.7 flares with 10:35 UT bursts, M1.7 flares with 13:17 UT bursts, and X1.5 flares with 23:13 UT bursts produced evident disturbances in the TEC images. This result verifies the conclusion drawn from this study when we investigated the sensitivity difference between TEC and VLF signals; that is, the lowest level of solar flares causing a strong disturbance to TEC is M-class flares, and the lowest level of solar flares causing a strong disturbance to VLF signals is C-class flares. The VLF phase demonstrates evident response to most C-class flares, particularly those with a long duration. For example, the duration of the C9.4 flare burst at 08:23 UT was 43 min, and evident changes can be observed from the phase images of VLF signals. This finding is consistent with the experimental results of Zhao and Wang [41] on the correlation between X-ray flux and VLF propagation phase shift during solar flares.

Although the sensitivity of ionospheric TEC and VLF signals to solar flares is different, they exhibit common characteristics in flare level, duration, geographical location, and local time. Figure 5 shows that the disturbance of VLF signals is closely related to local time. In this study, the TEC data of the JPLM Station on December 5, 2006 (Figure 6) and the TEC data of the ULAB Station on March 9, 2011 (Figure 8), as presented in Table 5, are comprehensively analyzed to verify further the close relationship between TEC and local time.

The JPLM station is located in West Area 8, and the ULAB station is located in West Area 7. In Table 5, flare time is converted into the local time of the station area. From the comparison of the two response data, the duration of the C3.7 and C5.7 flares in the morning is similar to that of the C9.4 flares in the afternoon, but the impact is considerably greater than the latter. Similarly, the flare of X9.0 that erupted near 02:00 local time and that of M1.8 that erupted at midnight are considerably less than those of X1.5 and M1.7 with the same level that erupted morning and night. The disturbance caused by flares in the morning of local time to TEC is larger than that in the afternoon. Moreover,

TABLE 5. The response of TEC data of JPLM and ULAB stations to different levels of flares at different local time.

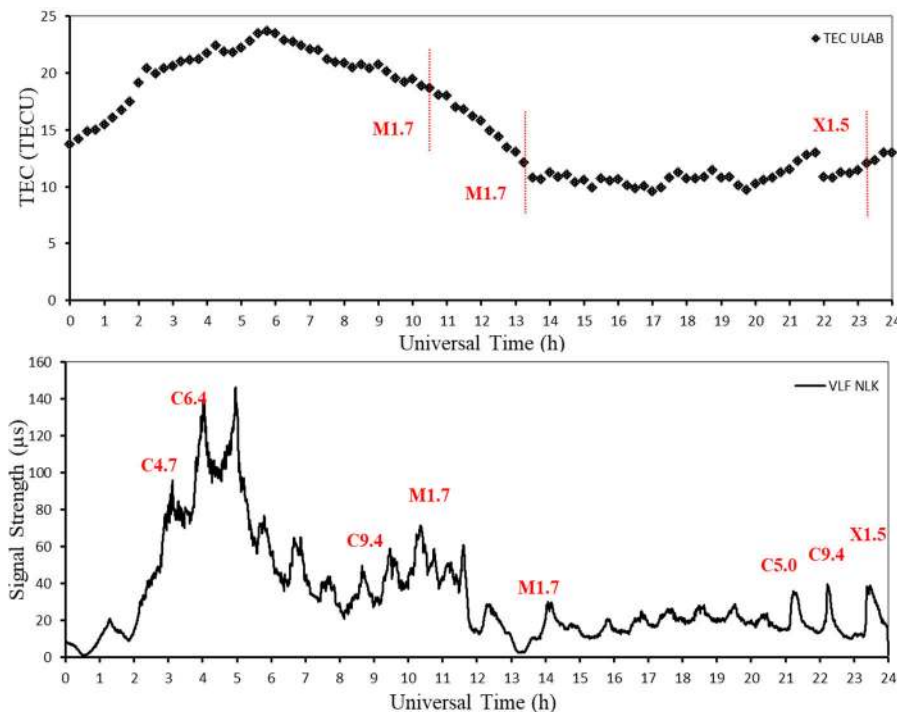| TEC Station	Local Time	Flare Class	Disturbance
JPLM	before dawn	X9.0	1.0 TECU
	forenoon	C3.7/C5.7	0.5 TECU
	midnight	M1.8	0.12 TECU
ULAB	morning	X1.5	2.0 TECU
	afternoon	C9.4	0.15 TECU
	night	M1.7	0.3 TECU

FIGURE 8. Images of TEC and VLF signals on March 9, 2011.

the disturbance of flares near the early morning of the local time to TEC is considerably smaller than that during daytime.

IV. CONCLUSION
On the basis of ionospheric TEC and VLF signals, this study comprehensively analyzes ionospheric response to solar flares of classes C–X on the day of the eruption of all X-class flares in 2006–2019. The following conclusions are drawn.

(1) In most cases, the higher the flare level, the greater the disturbance to TEC. The longer the duration of the flare, the greater the impact on TEC. Even for C-class and M-class flares, the impact on TEC may be great as long as the duration of the flare is long, showing the correctness of Chapman's theory. That is, the time change rate of ionospheric TEC is directly proportional to the effective radiation flux of solar flares. The higher the flare level and the longer the duration, the greater the disturbance effect on VLF signals.

(2) The disturbances of TEC and VLF signals are not only related to solar flares but also too many factors, such as geographical location and local time. The response of TEC and VLF signals from different stations to solar flares is different. The disturbance degree of the signals from a solar-facing station is considerably greater than that from the backside. DTEC tends to increase along Earth's rotation direction. The effect of solar flares erupting in the morning of the local time on the ionosphere is more evident than that erupting in the afternoon and the effect of flares erupting in the early morning of the local time is considerably smaller than that erupting during daytime. This result is consistent with the conclusion of Zhang and Xiao [42].

(3) The lowest flare level that causes TEC to respond strongly to solar flares is always at the M level. However, TEC also responding to several C-class flares with higher level and longer duration is not ruled out. Meanwhile, VLF signals can detect most C-class solar flares and produce different responses. At the same DI, the level of flares that causes TEC response is higher than that of VLF signals. The disturbance angle distribution range of TEC is [0°, 90°]. The disturbance angle of VLF signals is more than 85°, and thus, VLF signals are more sensitive to flares. The ionosphere response to solar flares is more accurate and reliable when VLF signals are used to monitor solar flares.

REFERENCES
[1] J. P. Eastwood, E. Biffis, M. A. Hapgood, L. Green, M. M. Bisi, R. D. Bentley, R. Wicks, L. A. McKinnell, M. Gibbs, and C. Burnett, "The economic impact of space weather: Where do we stand," *Risk Anal.*, vol. 37, no. 2, pp. 206–218, 2017.

[2] D. N. Baker, E. Daly, I. Daglis, J. G. Kappenman, and M. Panasyuk, "Effects of space weather on technology infrastructure," *Space Weather*, vol. 2, no. 2, pp. 1–11, Feb. 2004.

[3] A. Rozhnoi, M. Solovieva, V. Fedun, P. Gallagher, J. McCauley, M. Y. Boudjada, S. Shelyag, and H. U. Eichelberger, "Strong influence of solar X-ray flares on low-frequency electromagnetic signals in middle latitudes," *Annales Geophysicae*, vol. 37, no. 5, pp. 843–850, Sep. 2019.

[4] L. Qian, A. G. Burns, S. C. Solomon, and P. C. Chamberlin, "Solar flare impacts on ionospheric electrodyamics," *Geophys. Res. Lett.*, vol. 39, no. 6, pp. 151–153, 2012.

[5] C. S. Carrano, C. T. Bridgwood, and K. M. Groves, "Impacts of the December 2006 solar radio bursts on the performance of GPS," *Radio Sci.*, vol. 44, no. 1, pp. 1–12, 2009.

[6] S. Parmar, U. Dalal, and K. Pathak, "Analysing impact of major solar flares on ionospheric TEC with RTISM model using IRNSS receiver, at SVNIT, surat, india," *IET Commun.*, vol. 13, no. 18, pp. 2946–2955, Nov. 2019.

[7] D. H. Zhang, X. H. Mo, L. Cai, W. Zhang, M. Feng, Y. Q. Hao, and Z. Xiao, "Impact factor for the ionospheric total electron content response to solar flare irradiation," *J. Geophys. Res., Space Phys.*, vol. 116, no. A4, pp. 1–8, 2011.

[8] T. Mao, L. Sun, Y. Wang, C. She, B. Xiong, and L. Hu, "Response of the equatorial and low-latitude ionosphere over the west pacific ocean sector to an X1.2 solar flare on 15 may 2013," *Adv. Space Res.*, vol. 60, no. 5, pp. 1029–1038, Sep. 2017.

[9] W. G. Huang, S. F. Gu, Y. H. Chen, G. Y. Ma, and H. Shen, "The response of ionospheric TEC to small and faint solar flares," *Acta Astron. Sinica*, vol. 47, no. 2, pp. 212–217, 2006.

[10] H. Dahlgren, T. Sundberg, A. B. Collier, E. Koen, and S. Meyer, "Solar flares detected by the new narrowband VLF receiver at SANAE IV," *South Afr. J. Sci.*, vol. 107, nos. 9–10, pp. 1–8, Sep. 2011.

[11] A. Kumar and S. Kumar, "Solar flare effects on D-region ionosphere using VLF measurements during low- and high-solar activity phases of solar cycle 24," *Earth, Planets Space*, vol. 70, no. 1, pp. 1–14, Dec. 2018.

[12] A. Kolarski and D. Grubor, "Comparative analysis of VLF signal variation along trajectory induced by X-ray solar flares," *J. Astrophys. Astron.*, vol. 36, no. 4, pp. 1–15, Dec. 2015.

[13] M. A. Itkina, "Intensity of X-ray solar radiation and the value of the anomalous absorption of radio waves during periods of sudden ionospheric disturbances," *Radiophys. Quantum Electron.*, vol. 21, no. 11, pp. 1083–1086, Nov. 1978.

[14] N. R. Thomson, C. J. Rodger, and M. A. Clilverd, "Large solar flares and their ionospheric D region enhancements," *J. Geophys. Res., Space Phys.*, vol. 110, no. A6, 2005, Art. no. A06306.

[15] D. P. Grubor, D. M. Šulić, and V. Žigman, "Classification of X-ray solar flares regarding their effects on the lower ionosphere electron density profile," *Annales Geophysicae*, vol. 26, no. 7, pp. 1731–1740, Jun. 2008.

[16] W. T. Liu, "Correlative analysis between sudden phase anomalies of VIF signals and solar X-ray events," *Chin. J. Space Sci.*, vol. 7, no. 3, pp. 185–189, 1987.

[17] L. Loudet, "Application of empirical mode decomposition to the detection of sudden ionospheric disturbances by monitoring the signal of a distant very low frequency transmitter," *Creative Commons Version*, vol. 2, no. 5, 2009.

[18] W. M. Mcrae and N. R. Thomson, "Solar flare induced ionospheric D-region enhancements from VLF amplitude observations," *J. Atmos. Solar-Terr. Phys.*, vol. 66, no. 1, pp. 77–87, 2004.

[19] S. K. Chakrabarti, S. K. Mandal, S. Sasmal, D. Bhowmick, A. K. Choudhury, and N. N. Patra, "First VLF detections of ionospheric disturbances due to soft gamma ray repeater SGR J1550-5418 and gamma ray burst GRB 090424," *Indian J. Phys.*, vol. 84, no. 11, pp. 1461–1466, Nov. 2010.

[20] Y. T. Tanaka, J.-P. Raulin, F. C. P. Bertoni, P. R. Fagundes, J. Chau, N. J. Schuch, M. Hayakawa, Y. Hobara, T. Terasawa, and T. Takahashi, "First very low frequency detection of short repeated bursts from magnetar SGR J1550–5418," *Astrophys. J.*, vol. 721, no. 1, pp. L24–L27, Sep. 2010.

[21] H. E. George, C. J. Rodger, M. A. Clilverd, K. Cresswell-Moorcock, J. B. Brundell, and N. R. Thomson, "Developing a nowcasting capability for X-class solar flares using VLF radiowave propagation changes," *Space Weather*, vol. 17, no. 12, pp. 1783–1799, Dec. 2019.

[22] R. Vogrinčič, A. Lara, A. Borgazzi, and J. P. Raulin, "Effects of the great American solar eclipse on the lower ionosphere observed with VLF waves," *Adv. Space Res.*, vol. 65, no. 9, pp. 2148–2157, May 2020.

[23] S. Palit, T. Basak, S. Pal, and S. K. Chakrabarti, "Theoretical study of lower ionospheric response to solar flares: Sluggishness of D-region and peak time delay," *Astrophys. Space Sci.*, vol. 356, no. 1, pp. 19–28, Mar. 2015.

[24] S. Palit, S. Ray, and S. K. Chakrabarti, "Inverse problem in ionospheric science: Prediction of solar soft-X-ray spectrum from very low frequency radiosonde results," *Astrophys. Space Sci.*, vol. 361, no. 5, pp. 1–11, May 2016.

[25] F. Arikan, "Regularized estimation of vertical total electron content from global positioning system data," *J. Geophys. Res.*, vol. 108, no. A12, p. 1469, 2003.

[26] F. Arikan, O. Arikan, and C. B. Erol, "Regularized estimation of TEC from GPS data for certain midlatitude stations and comparison with the IRI model," *Adv. Space Res.*, vol. 39, no. 5, pp. 867–874, 2007.

[27] F. Arikan, C. B. Erol, and O. Arikan, "Regularized estimation of vertical total electron content from GPS data for a desired time period," *Radio Sci.*, vol. 39, no. 6, pp. 1–10, Dec. 2004.

[28] H. Nayir, F. Arikan, O. Arikan, and C. B. Erol, "Total electron content estimation with Reg-Est: TEC estimation With Reg-Est," *J. Geophys. Res., Space Phys.*, vol. 112, no. A11, Nov. 2007, Art. no. A11313.

[29] F. Arikan, H. Nayir, U. Sezen, and O. Arikan, "Estimation of single station interfrequency receiver bias using GPS-TEC," *Radio Sci.*, vol. 43, no. 4, Aug. 2008, Art. no. RS4004.

[30] U. Sezen, F. Arikan, O. Arikan, O. Ugurlu, and A. Sadeghimorad, "Online, automatic, near-real time estimation of GPS-TEC: IONOLAB-TEC: Online GPS-TEC: IONOLAB-TEC," *Space Weather*, vol. 11, no. 5, pp. 297–305, May 2013.

[31] A. Komjathy, "Global ionospheric total electron content mapping using the Global Positioning System," Ph.D. dissertation, Univ. New Brunswick, Fredericton, NB, Canada, 1997.

[32] S. Schaer, "Mapping and predicting the Earth's ionosphere using the Global Positioning System," Ph.D. dissertation, Astron. Inst., Univ. Bern, Bern, Switzerland, 1999.

[33] S. A. Bahari, M. Abdullah, and B. Yatim, "The response of TEC at quasi-conjugate point GPS stations during solar flares," *Acta Geophys.*, vol. 59, no. 2, pp. 407–419, Apr. 2011.

[34] B. Chen, L. Liu, W. Wan, B. Ning, and F. Ding, "Statistical analysis of TEC sudden enhancement caused by the great flare event in 1996–2003," *J. Space Sci.*, vol. 25, no. 1, pp. 6–16, 2005.

[35] E. L. Afraimovich, A. T. Altynsev, V. V. Grechnev, and L. A. Leonovich, "Ionospheric effects of the solar flares as deduced from global GPS network data," *Adv. Space Res.*, vol. 27, nos. 6–7, pp. 1333–1338, Jan. 2001.

[36] H. Le, L. Liu, B. Chen, J. Lei, X. Yue, and W. Wan, "Modeling the responses of the middle latitude ionosphere to solar flares," *J. Atmos. Solar-Terr. Phys.*, vol. 69, no. 13, pp. 1587–1598, Sep. 2007.

[37] T. Basak and S. K. Chakrabarti, "Effective recombination coefficient and solar zenith angle effects on low-latitude D-region ionosphere evaluated from VLF signal amplitude and its time delay during X-ray solar flares," *Astrophys. Space Sci.*, vol. 348, no. 2, pp. 315–326, Dec. 2013.

[38] L. A. Hayes, P. T. Gallagher, J. McCauley, B. R. Dennis, J. Ireland, and A. Inglis, "Pulsations in the Earth's lower ionosphere synchronized with solar flare emission," *J. Geophys. Res., Space Phys.*, vol. 122, no. 10, pp. 9841–9847, Oct. 2017.

[39] A. Sharma and C. More, "Diurnal variation of VLF radio wave signal strength at 19.8 and 24 kHz received at Khatav India (16046'N, 75053'E)," *Res. Rev., J. Space Sci. Technol.*, vol. 6, no. 2, pp. 1–12, 2017.

[40] Y. Zhu, W. Zong, and S. Pei, "Study on the relationship between flares above X level and geomagnetic effect," *J. Acta Space Sci.*, vol. 35, no. 4, pp. 415–423, 2015.

[41] X. Zhao and X. Wang, "The study of correlation between VLF phase anomalies and solar X-ray fluxes during solar flares," *Chin. J. Radio Sci.*, vol. 5, no. 2, pp. 35–43, 1990.

[42] D. Zhang and Z. Xiao, "Analysis of GPS observation results of ionospheric TEC during the great flare on November 6, 1997," *Chin. Sci. Bull.*, no. 6, pp. 575–578, 2000.

JIANDI FENG received the Ph.D. degree from Wuhan University. He is currently a Lecturer with the Shandong University of Technology. His current research interests include GNSS data processing and ionospheric empirical modeling.

BAOMIN HAN received the Ph.D. degree from the Institute of Geodesy and Geophysics, Chinese Academy of Sciences. He is currently a Professor with the Shandong University of Technology, where he serves as the Assistant Dean of the School of Civil and Architectural Engineering. His current research interests include GNSS precise positioning and low orbit satellite precise orbit determination.

TING ZHANG is currently pursuing the master's degree in surveying and mapping with the Shandong University of Technology. His main research interests include GNSS data processing and ionospheric empirical modeling.

FENG GAO is currently pursuing the bachelor's degree in surveying and mapping engineering with the Shandong University of Technology. His main research interest includes ionospheric empirical modeling.

ZHENZHEN ZHAO received the Ph.D. degree from Wuhan University. She is currently a Lecturer with the Shandong University of Technology. Her current research interests include environmental remote sensing and change monitoring.

• • •